

Research Article

Effects of Vertical Transmission and Human Contact on Zika Dynamics

Abdoulaye Sow ¹, Cherif Diallo ¹, and Hocine Cherifi ²

¹University Gaston Berger, Saint-Louis, Senegal

²University of Burgundy, Dijon, France

Correspondence should be addressed to Abdoulaye Sow; sow.abdoulaye6@ugb.edu.sn

Received 11 September 2021; Revised 14 February 2022; Accepted 16 February 2022; Published 17 March 2022

Academic Editor: Siew Ann Cheong

Copyright © 2022 Abdoulaye Sow et al. This is an open access article distributed under the Creative Commons Attribution License, which permits unrestricted use, distribution, and reproduction in any medium, provided the original work is properly cited.

The main objective of Zika transmission studies is to work out the simplest approach to scale back human mortality and morbidity caused by the disease. Therefore, it is essential to spot the relative importance of the various factors contributing to the transmission and prevalence of the disease. Many mathematical models have been formulated incorporating vector-to-human transmission or human-to-human transmission. However, they do not take into consideration the mixture of both sorts of transmission. It raises the question of the impact of both sorts of transmission on the disease dynamics. We develop a mathematical model of Zika with the vertical transmission in the vector population and human-to-human transmission to answer this question. It includes the immature phase of mosquitoes (eggs), adult mosquitoes (susceptible, exposed, and infectious), and human hosts (susceptible, exposed, infectious, and recovered). Results show that neglecting sexual transmission results in an understatement of the proportion of the infected population. Furthermore, it reduces the speed of disease spreading. On the other hand, vertical transmission in mosquitoes has a negligible effect on the dynamics of disease spread. We perform a sensitivity analysis of the reproductive number R_0 to raise to understand the parameters driving the dynamics of the disease. It appears that the most sensitive parameters in decreasing order are as follows: the adult mosquito death rate, the sting rate, the transmission probability of mosquito to human, and, therefore, the transmission probability of human to mosquito. Furthermore, the proportion at the equilibrium of infected humans is extremely sensitive to the transition rate from the immature vector stage to the adult stage, the human-to-human transmission rate, and, therefore, the human recovery rate. These results confirm that control policies targeting the vector population and, therefore, the recovery rate of people are pretty effective solutions. To validate the model and estimate the important parameters of the model and the prediction of the disease, we consider the real cases in Colombia from 2016. In a series of graphic maps, we presented the comparative study to estimate the disease scenarios and to predict the time limit of the epidemic control measure.

1. Introduction

Zika is an infectious disease transmitted by *Aedes* mosquitoes. This virus belongs to the genus of Flaviviruses, such as dengue and West Nile. The disease first appeared in Uganda in 1947. The first human cases occurred in the 1970s in other African countries (Tanzania, Egypt, Central African Republic, Sierra Leone, Gabon, and Senegal) and some Asian countries (India, Malaysia, Philippines, Thailand, Vietnam, and Indonesia). In 2007, a real epidemic broke out in Micronesia (Yap Island in the Pacific) [1], causing 5,000

infections. In 2013 and 2014, 55,000 cases have been reported in French Polynesia [2]. The epidemic then spread to other Pacific islands, including New Caledonia, the Cook Islands, and Easter Island. Zika was first detected in northwestern Brazil in May 2015, rapidly spreading to other parts of the country [3]. Brazil reported the highest number of cases: between 440,000 and 1,500,000 suspected cases. Since 2016, Zika has been included in the World Health Organization (WHO) priority disease list for research and development. It is one of the main concerns of public health organizations around the world [4]. In this context, various mathematical

models of Zika dynamics have been developed. In [5], Towers et al. introduce a compartmentalized model incorporating a susceptible-exposed-infected-removed (SEIR) model for the host population and a susceptible-exposed-infected (SEI) model for vectors. They estimate the reproduction number ($R_0 = 3.8$), and the fraction of cases due to sexual transmission is equal to 0.23. In [6], Soriano-Paños et al. propose a compartmental model that takes into account human mobility and demographics. They derive an expression for the epidemic threshold capturing the conditions of the epidemic outbreak and identify some invisible characteristics of vector-borne epidemics, such as abrupt changes in disease patterns for small changes in the degree of mobility. In addition, information on the sexual transmission of the Zika virus is based on a few cases of transmission from men to their partners [7, 8]. Since then, several mathematical models introducing direct human-to-human transmission have been documented by researchers. The first study of the effect of sexual transmission in the human population is due to Gao et al. [9]. They show that sexual transmission has a minor influence on the basic reproduction rate, but it can increase the risk of infection and disease size. In [10], Arquam et al. formulated a direct transmission model with a heterogeneous contact network that takes into account the effect of seasonality influence on vectors. Their research has shown that failure to incorporate these characteristics into the model can lead to underestimating the maximum fraction of infected individuals in the host population. In addition, the time required to reach the peak of the infection is very sensitive to these variations. In [11], Suparit et al. developed a model that takes into account the time dependence of the mosquito bite rate. They show that the simulation results of their model can be very consistent with data reported in Bahia in 2016. In [12], Augusto et al. examined the importance of vertical transmission of the virus in humans in addition to transmission of the disease through mosquito bites. They show that mosquito demographic parameters and human-mosquito transmission parameters play an essential role in the spread of Zika.

In contrast to previous studies that focused on at most two transmission routes of ZIKV, we introduce a new mathematical model that integrates (1) sexual transmission and (2) vertical transmission of ZIKV within mosquito populations. By analyzing the simultaneous transmission cycles of ZIKV in human and vector populations, we aim to answer the following research question: what is the relative contribution of individual and combined transmission mechanisms on the spread of Zika? Quantifying the effects of these transmission pathways contributes to a better understanding of the overall population dynamics of Zika and is also a precious aid in designing effective control strategies. This study makes an essential contribution to the existing knowledge about Zika. Indeed, we propose a compartmental model for Zika transmission that integrates both horizontal transmission in the host population and vertical transmission in vectors. In the case of human-human transmission, it considers the number of contacts per day (k) using the homogeneous mean-field approach. The resulting model can

reproduce results that allow us to better understand the maximum number of infections for each transmission type and the time to reach the peak of the disease. In addition, we study how the different parameters of secondary transmission pathways affect Zika R_0 estimates. The last section is devoted to exploiting the data to recover epidemic parameters, such as the rate of human-to-human transmission and the rate of vertical transmission in vectors. The model would also be validated by comparing the model's prediction with data reported in Colombia in 2016.

2. Methodology

Figure 1 presents the block diagram illustrating the vector-host and the host-host interactions in the SEIR-SEI-SI model. It describes the compartmental classifications used to simulate the transmission dynamics of ZIKV. The model integrates two types of populations: the human and vector populations. The human population is in one of the four epidemiological states: susceptible (S_h), exposed (E_h), infectious (I_h), and recovered (R_h). The vector population contains mosquitoes and eggs. Mosquitoes are in one of the three epidemiological classes: susceptible (S_v), exposed (E_v), and infectious (I_v). Eggs are in one of the two epidemiological classes: susceptible (S_e) and infected (I_e). The model incorporates human-to-human transmission and vertical transmission by mosquitoes. Two transmission routes can infect a healthy host: (1) a bite by an infected vector and (2) direct interaction with an infected host. A healthy vector can become infected after feeding on an infected person.

After infection with ZIKV, a person incubates the virus at a rate α_h before becoming infectious. Infected persons recover at a rate of γ_h . We assume that they have lifelong immunity after recovery. Susceptible adult female mosquitoes contract ZIKV after feeding on an infected person. These exposed mosquitoes can then become infectious at a rate α_v . This rate is inversely proportional to the extrinsic incubation period.

In contrast to humans, infectious mosquitoes remain infectious throughout their lifespan. Eggs are either susceptible or infected. Infected eggs can hatch into either an infected mosquito or an uninfected mosquito.

We also assume that the human population is homogeneous. In other words, each individual has, on average, the same number of contacts, k . It allows us to disentangle the effect of vertical transmission from complementary phenomena. The total number of the host, vector, and egg populations at time t is given, respectively, by given by $N_h(t)$, $N_v(t)$, and $N_e(t)$, respectively, such that:

$$\begin{aligned} N_h(t) &= S_h(t) + E_h(t) + I_h(t) + R_h(t), \\ N_v(t) &= S_v(t) + E_v(t) + I_v(t), \\ N_e(t) &= S_e(t) + I_e(t). \end{aligned} \quad (1)$$

Figure 1 shows the compartmental diagram based on these assumptions. The parameters indicated in Figure 1 are described in Table 1.

Based on the assumptions and the interrelations between the variables and the parameters as shown in the model

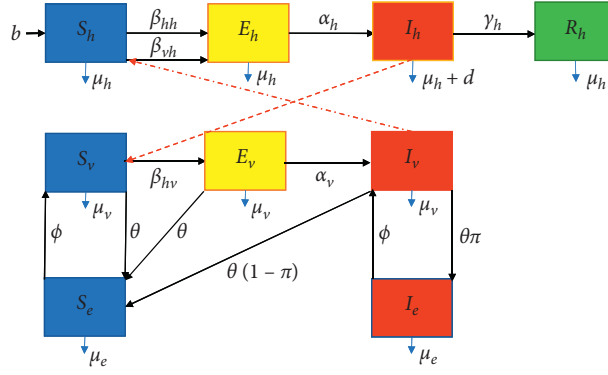


FIGURE 1: The flowchart represents the interactions and transfer of vector-borne disease in both human and vector populations. The host population is split into the following states: susceptible S_h , exposed E_h , infectious I_h , and recovered R_h . The vector population is split into three states: susceptible S_v , exposed E_v , and infectious I_v . The egg population is split into two states: susceptible S_e and infectious I_e . Dashed arrows show the direction of transmission between humans and mosquitoes.

compartments in Figure 1, the effect of transmission of human to human and vertical transmission on vector-borne

disease transmission dynamics can be described by the ordinary differential (2).

$$\begin{aligned}
 \frac{dS_h(t)}{dt} &= bN_h - k\beta_{hh}\frac{S_h(t)I_h(t)}{N_h(t)} - a\beta_{vh}\frac{S_h(t)I_v(t)}{N_h(t)} - \mu_h S_h(t), \\
 \frac{dE_h(t)}{dt} &= k\beta_{hh}\frac{S_h(t)I_h(t)}{N_h(t)} + a\beta_{vh}\frac{S_h(t)I_v(t)}{N_h(t)} - \alpha_h E_h(t) - \mu_h E_h(t), \\
 \frac{dI_h(t)}{dt} &= \alpha_h E_h(t) - \gamma_h I_h(t) - \mu_h I_h(t) - dI_h(t), \\
 \frac{dR_h(t)}{dt} &= \gamma_h I_h(t) - \mu_h R_h(t), \\
 \frac{dS_v(t)}{dt} &= \phi S_e(t) - a\beta_{hv}\frac{I_h(t)S_v(t)}{N_h(t)} - \mu_v S_v(t), \\
 \frac{dE_v(t)}{dt} &= a\beta_{hv}\frac{S_v(t)I_h(t)}{N_h(t)} - \alpha_v E_v(t) - \mu_v E_v(t), \\
 \frac{dI_v(t)}{dt} &= \phi I_e(t) + \alpha_v E_v(t) - \mu_v I_v(t), \\
 \frac{dS_e(t)}{dt} &= \theta N_v(t) - \pi\theta I_v(t) - \phi S_e(t) - \mu_e S_e(t), \\
 \frac{dI_e(t)}{dt} &= \pi\theta I_v(t) - \phi I_e(t) - \mu_e I_e(t).
 \end{aligned} \tag{2}$$

TABLE 1: Values of parameters used in the model, and the sources used for the numerical values.

Parameter	Definition	Value	Source
β_{hv}	Infection incidence rate from host to vector	0.5	[13]
a	Per capita contact (biting) rate	0.5	[14]
β_{vh}	Infection incidence rate from vector to host	0.4	[14]
β_{hh}	Infection incidence rate from host to host	0.3	Assumed
α_h^{-1}	Incubation rate of a host	5.9	[15]
γ_h^{-1}	Human infectivity period (days)	5	[15]
μ_h	Natural mortality rate of humans	0.000 04	[16]
d	Disease-induced mortality rate of humans	0.01	[16]
α_v	Incubation rate of a vector	0.1	[17]
μ_v^{-1}	Mosquito lifespan (days)	14	[14]
θ	Number of Aedes eggs laid per day	0.005	[18]
π	Vertical transmission rate	0.05	[19]
ϕ	Development rate of mosquitoes	0.19	[20]
b	Daily human recruitment rate	0.000 1	Assumed
μ_e	Natural mortality rate of eggs	0.2	[21]

3. Disease-Free Equilibria

To simplify the calculation of R_0 , we rewrite the system in the following form:

$$\begin{aligned}
\frac{ds_h(t)}{dt} &= b - k\beta_{hh}s_h(t)i_h(t) - a\beta_{vh}s_h(t)i_v(t) - \mu_h s_h(t), \\
\frac{de_h(t)}{dt} &= k\beta_{hh}s_h(t)i_h(t) + a\beta_{vh}s_h(t)i_v(t) - \alpha_h e_h(t) - \mu_h e_h(t), \\
\frac{di_h(t)}{dt} &= \alpha_h e_h(t) - \gamma_h i_h(t) - \mu_h i_h(t) - di_h(t), \\
\frac{dr_h(t)}{dt} &= \gamma_h i_h(t) - \mu_h r_h(t), \\
\frac{ds_v(t)}{dt} &= \phi s_e(t) - a\beta_{hv}i_h(t)s_v(t) - \mu_v s_v(t), \\
\frac{de_v(t)}{dt} &= a\beta_{hv}s_v(t)i_h(t) - (\alpha_v + \mu_v)e_v(t), \\
\frac{di_v(t)}{dt} &= \phi i_e(t) + \alpha_v e_v(t) - \mu_v i_v(t), \\
\frac{ds_e(t)}{dt} &= \theta(1 - \pi i_v(t)) - \phi s_e(t) - \mu_e s_e(t), \\
\frac{di_e(t)}{dt} &= \theta \pi i_v(t) - \phi i_e(t) - \mu_e i_e(t).
\end{aligned} \tag{3}$$

The disease-free equilibrium is the point with no disease is in the population. To find the disease-free equilibrium of the proposed model (1), we set the right-hand side of all equations equal to zero and

$$e_h = i_h = e_v = i_v = 0. \tag{4}$$

Therefore, the disease-free equilibrium (DFE) is given by the following:

$$E_0 = \left(k \frac{b}{\mu_h}, 0, 0, 0, \frac{\phi}{\mu_v}, 0, 0, \frac{\theta}{\phi + \mu_e}, 0 \right). \tag{5}$$

The basic reproduction number R_0 of the model is computed using the next-generation matrix approach. It is

the dominant eigenvalue or spectral radius of the next-generation matrix FV^{-1} , where

$$F = \begin{pmatrix} 0 & k\beta_{hh}\frac{b}{\mu_h} & 0 & a\beta_{vh}\frac{b}{\mu_h} & 0 \\ 0 & 0 & 0 & 0 & 0 \\ 0 & a\beta_{hv}\frac{\phi}{\mu_v} & 0 & 0 & 0 \\ 0 & 0 & 0 & 0 & 0 \\ 0 & 0 & 0 & 0 & 0 \end{pmatrix}, \quad (6)$$

$$V = \begin{pmatrix} \alpha_h + \mu_h & 0 & 0 & 0 & 0 \\ -\alpha_h & \gamma_h + d + \mu_h & 0 & 0 & 0 \\ 0 & 0 & \alpha_v + \mu_v & 0 & 0 \\ 0 & 0 & -\alpha_v & \mu_v & -\phi \\ 0 & 0 & 0 & -\pi\theta & \phi + \mu_e \end{pmatrix}.$$

The inverse of the matrix V is given by the following:

$$V^{-1} = \begin{pmatrix} \frac{1}{\alpha_h + \mu_h} & 0 & 0 & 0 & 0 \\ \frac{\alpha_h}{(\alpha_h + \mu_h)(\gamma_h + d + \mu_h)} & \frac{1}{\gamma_h + d + \mu_h} & 0 & 0 & 0 \\ 0 & 0 & \frac{1}{\alpha_v + \mu_v} & 0 & 0 \\ 0 & 0 & \frac{\alpha_v(\phi + \mu_e)}{(\alpha_v + \mu_v)(\mu_v(\phi + \mu_e) - \phi\pi\theta)} & \frac{\phi + \mu_e}{\mu_v(\phi + \mu_e) - \phi\pi\theta} & \frac{\phi}{\mu_v(\phi + \mu_e) - \phi\pi\theta} \\ 0 & 0 & \frac{\alpha_v\pi\theta}{(\alpha_v + \mu_v)(\mu_v(\phi + \mu_e) - \phi\pi\theta)} & \frac{\pi\theta}{\mu_v(\phi + \mu_e) - \phi\pi\theta} & \frac{\mu_v}{\mu_v(\phi + \mu_e) - \phi\pi\theta} \end{pmatrix}. \quad (7)$$

Now we have to compute FV^{-1} .

$$FV^{-1} = \begin{pmatrix} F_{12}A_{21} & F_{12}A_{22} & F_{14}A_{43} & F_{14}A_{44} & F_{14}A_{45} \\ 0 & 0 & 0 & 0 & 0 \\ F_{32}A_{21} & F_{32}A_{23} & 0 & 0 & 0 \\ 0 & 0 & 0 & 0 & 0 \\ 0 & 0 & 0 & 0 & 0 \end{pmatrix}. \quad (8)$$

Such as $F_{12} = k\beta_{hh}b/\mu_h$, $F_{14} = a\beta_{vh}b/\mu_h$, $F_{32} = a\beta_{hv}\phi/\mu_v$, $A_{11} = 1/\alpha_h + \mu_h$, and $A_{21} = \alpha_h/(\alpha_h + \mu_h)(\gamma_h + d + \mu_h)$,

$$\begin{aligned} A_{22} &= \frac{1}{\gamma_h + d + \mu_h}, \\ A_{33} &= \frac{1}{\alpha_v + \mu_v}, \\ A_{43} &= \frac{\alpha_v(\phi + \mu_e)}{(\alpha_v + \mu_v)(\mu_v(\phi + \mu_e) - \phi\pi\theta)}, \\ A_{44} &= \frac{\phi + \mu_e}{\mu_v(\phi + \mu_e) - \phi\pi\theta}, \\ A_{45} &= \frac{\phi}{\mu_v(\phi + \mu_e) - \phi\pi\theta}, \\ A_{53} &= \frac{\alpha_v\pi\theta}{(\alpha_v + \mu_v)(\mu_v(\phi + \mu_e) - \phi\pi\theta)}, \\ A_{54} &= \frac{\pi\theta}{\mu_v(\phi + \mu_e) - \phi\pi\theta}, \\ A_{55} &= \frac{\mu_v}{\mu_v(\phi + \mu_e) - \phi\pi\theta}. \end{aligned} \quad (9)$$

From the above matrix, we can now calculate the eigenvalues to determine the basic reproduction number R_0 by taking the spectral radius (dominant eigenvalue) of the matrix FV^{-1} .

Thus, it is computed by $|\lambda I - FV^{-1}| = 0$. The characteristic equation is given as follows:

$$-\lambda^3(-F_{12}A_{21}\lambda - F_{14}A_{43}F_{32}A_{21} + \lambda^2) = 0. \quad (10)$$

The dominant eigenvalue of the matrix FV^{-1} is

$$\lambda = \frac{F_{12}A_{21} + \sqrt{(F_{12}A_{21})^2 + 4F_{14}A_{43}F_{32}A_{21}}}{2}. \quad (11)$$

Therefore, the basic reproduction number is given by the following:

$$\begin{aligned} R_0 &= \frac{F_{12}A_{21} + \sqrt{(F_{12}A_{21})^2 + 4F_{14}A_{43}F_{32}A_{21}}}{2}, \\ R_0 &= \frac{R_{hh} + \sqrt{R_{hh}^2 + 4R_{hv}}}{2}, \end{aligned} \quad (12)$$

where

$$R_{hh} = k \frac{b\alpha_h\beta_{hh}}{\mu_h(\alpha_h + \mu_h)(\mu_h + \gamma_h + d)}, \quad (13)$$

$$R_{hv} = \frac{a^2b\alpha_h\alpha_v\phi(\phi + \mu_e)\beta_{vh}\beta_{hv}}{\mu_v\mu_h(\alpha_h + \mu_h)(\gamma_h + d + \mu_h)(\alpha_v + \mu_v)(\mu_v(\phi + \mu_e) - \phi\pi\theta)}. \quad (14)$$

Equation (12) represents the average number of secondary cases generated by an individual during the period of infectiousness when introducing a Zika infection into a fully

susceptible population. It is called the basic reproduction rate (R_0). If its value is less than 1, each case gives fewer than one secondary case on average. Therefore, the number of cases decreases with each generation, and the chain of transmission eventually breaks down. Conversely, if $R_0 > 1$, the number of cases increases with each generation creating an epidemic.

4. Numerical Simulations

To visualize the difference between the dynamics of the vector model only (i.e., a model that considers the transmission between vector and human only) and our model, we perform numerical simulations using MATLAB. The values of the parameters used in the simulations are reported in Table 1.

Figure 2 shows the dynamics of disease spread with the SEIR-SEI model with vector contamination alone. The susceptible population decreases from the start to day 80. The size of the infected population increases until quite rapidly it reaches a peak of 15% of the people. Then, it gradually decreases. This process ends after 75 days when the entire host population recovers.

Figure 3 shows the dynamics of the SEIR-SEI model with two transmission routes (vector-to-human and human-to-human transmission). We use the same set of parameters as in the previous experiment for comparison. We find that with the model with the human-to-human transmission, the peak infection of the disease is 1.2 times higher than with the model with vector transmission only.

As expected, the epidemic affects more people and has a more significant impact on the initial growth of the disease than when there is a single transmission route.

Figure 4 shows the spread of the epidemic in the host population with the same set of parameters as used in the simulation in Figure 2. The only difference is that, in this case, the vertical transmission at the vector level is taken into account. One can see that the infection spreads to a maximum and then gradually decreases over 60 days. In addition, the proportion of infected hosts is much higher, with a maximum number of 21% of the population infected compared to 15% in the model without vertical transmission. The main lesson learned thus far is that neglecting to think about the influence of secondary transmission within the dynamics of the epidemic can cause an understatement of the proportion of the population, which will be infected and, therefore, the speed of transmission of the disease.

Figure 5 shows the spread of the epidemic in the host population under the same conditions as in the previous experiments. Except here, we consider a complete model, i.e., a vector-human model influencing both human-to-human transmission and vertical transmission in mosquitoes. We observe the most rapid infection growth in the human population in this model than in the single-vector model. Indeed, ZIKV infects about 23% of the people at the peak of the epidemic. This peak is reached two weeks earlier than in the single-vector model. One can conclude that employing a vector-only transmission model rather than an entire model may cause an underestimation of the

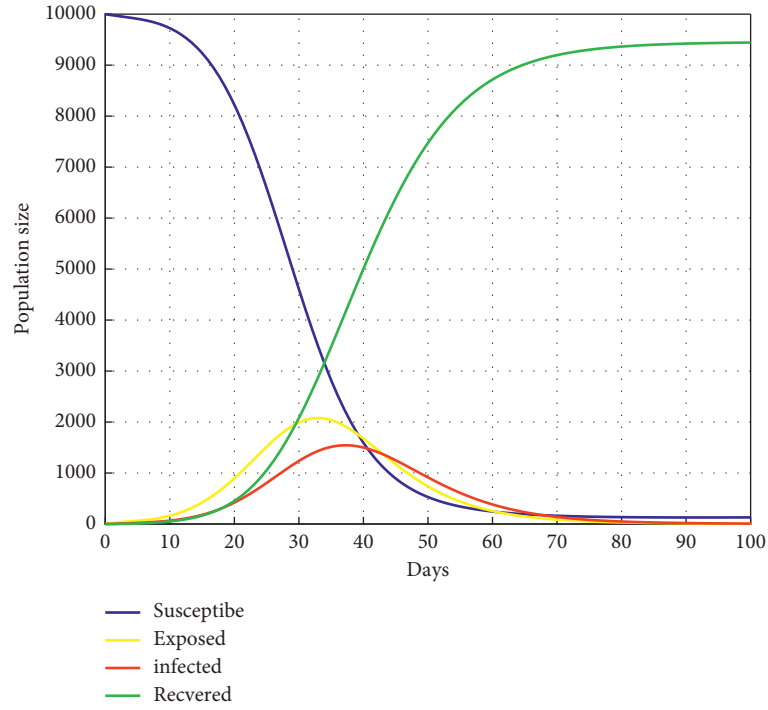


FIGURE 2: Evolution of the epidemic spreading considering the transmission vector-to-human transmission route only, i.e., infection incidence rate from host to host $\beta_{hh} = 0$ and vertical transmission rate $\pi = 0$.

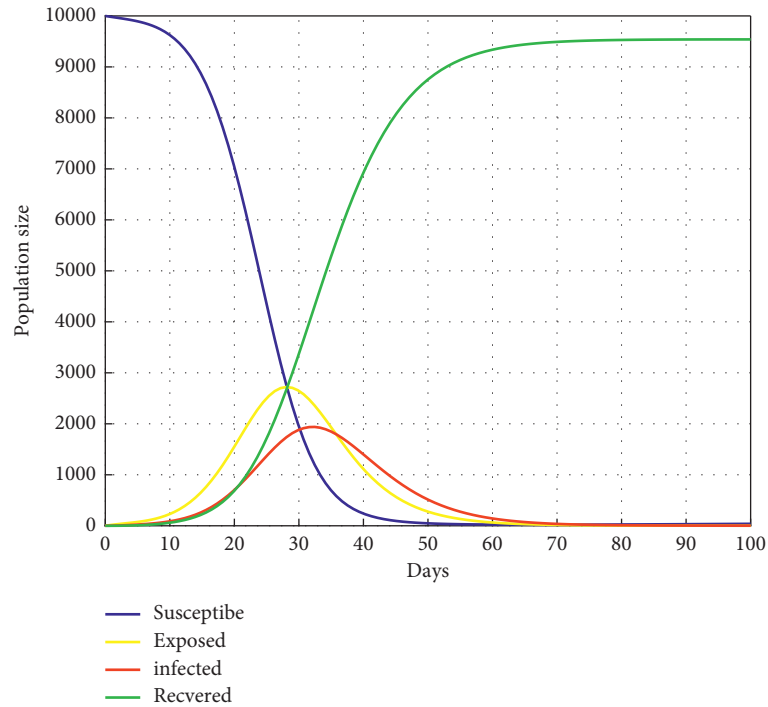


FIGURE 3: Evolution of the epidemic spreading considering the vector-to-human and the human-to-human transmission routes, i.e., vertical transmission rate $\pi = 0$.

proportion of the population infected and, therefore, the speed of disease spreading. These results could also be of great interest to public health officials who use predictive modeling tools to work out the timing and intensity of

control strategies. Indeed, one can exploit the differences between the vector-only model and, therefore, the full model to style effective control strategies tailored to the transmission patterns.

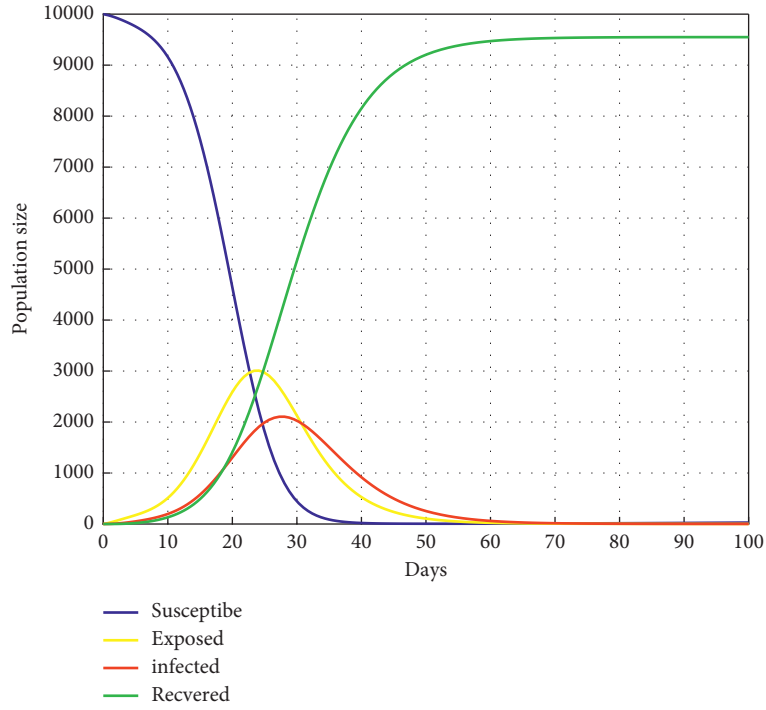


FIGURE 4: Evolution of the epidemic spreading considering the vector-to-human transmission route and mosquito vertical transmission, i.e., infection incidence rate from host to host $\beta_{hh} = 0$.

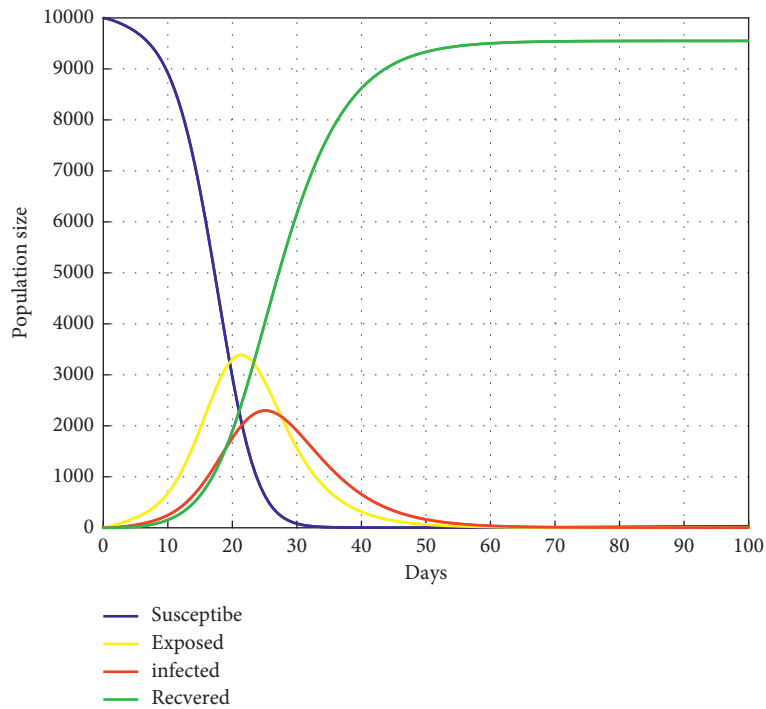


FIGURE 5: Evolution of the epidemic spreading considering the full model.

We further assess the impact of human-to-human transmission and vector-to-human transmission with simulations of the whole model. To do so, we use various values for the parameters β_{hh} and β_{vh} , and the remaining parameters are the ones reported in Table 1. The results represented

in Figure 6 show, as expected, that the number of infected persons increases with increasing values of β_{hh} . Similarly, increasing the value of the parameter β_{vh} increases the number of infected people as illustrated in Figure 7. Note that the peaks of infection differ in Figures 6 and 7. Indeed,

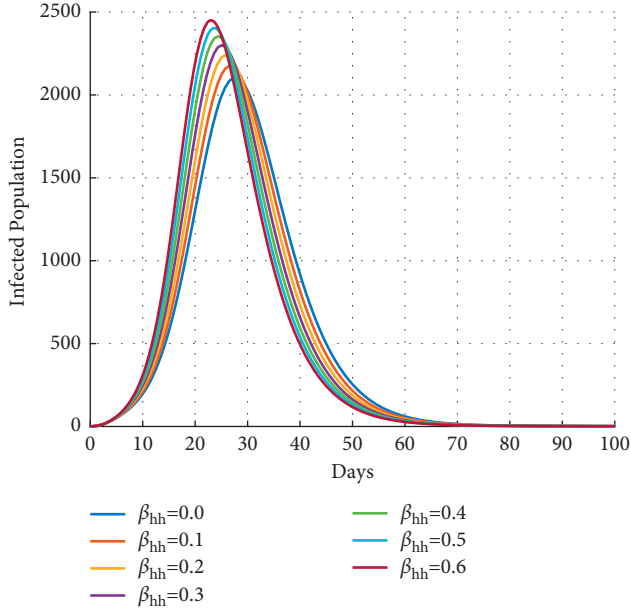


FIGURE 6: Evolution of the epidemic spreading in the host population for various values of the host-to-host transmission rate β_{hh} .

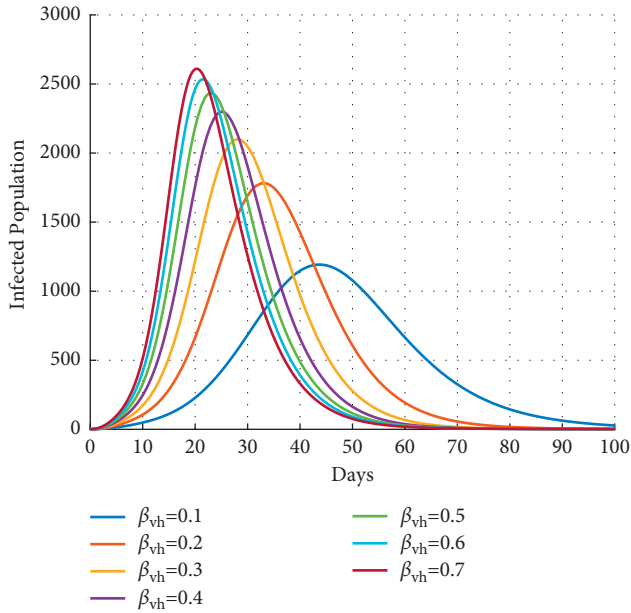


FIGURE 7: Evolution of the epidemic spreading in the vector population for various values of the vector-to-host transmission rate β_{vh} .

the infection size and rate more rapidly vary in Figure 7 than in Figure 6.

The value of the maximum proportion of infected individuals $I_{h_{\max}}$ at time t_{\max} in the host population with the variation of β_{hh} and β_{vh} is given in Tables 2 and 3.

Figures 8 and 9 illustrate the epidemic dynamics in the vector population. Figure 8 shows that, without human-mosquito interaction, vertical transmission (π) has a very marginal effect on the abundance of infected adult female

TABLE 2: Influence of the host-to-host transmission rate β_{hh} on the maximum proportion of infected individuals in the host population $I_{h_{\max}}$ at time t_{\max} .

β_{hh}	0	0.1	0.2	0.3	0.4	0.5	0.6
$I_{h_{\max}}$	2128	2176	2234	2300	2351	2402	2453
t_{\max}	28	27	26	25	24	23	22

TABLE 3: Influence of the vector-to-host transmission rate β_{vh} on the maximum proportion of infected individuals in the host population $I_{h_{\max}}$ at time t_{\max} .

β_{vh}	0.1	0.2	0.3	0.4	0.5	0.6	0.7
$I_{h_{\max}}$	1193	1781	2102	2292	2438	2532	2611
t_{\max}	43	33	28	25	23	21	20

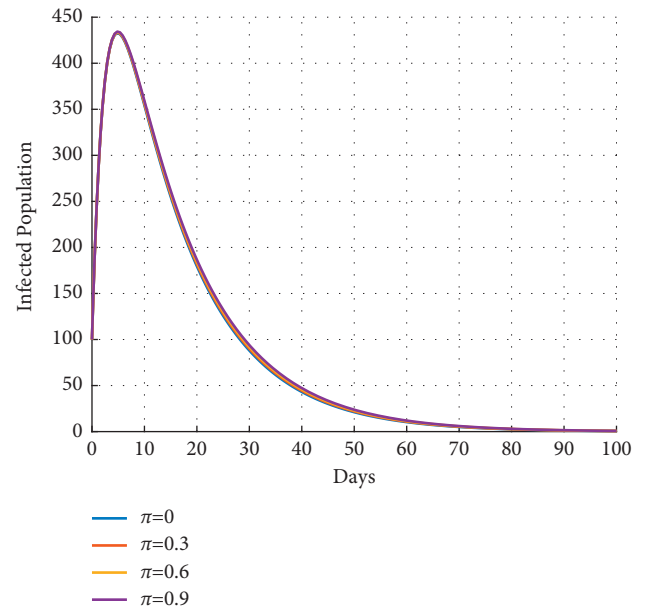


FIGURE 8: Evolution of the epidemic spreading in the vector population for various values of the vertical transmission rate π . Mosquito-to-human interaction is set at $a = 0$.

mosquitoes. However, when human-mosquito interaction marginally increases (such as by setting the biting rate to $a = 0.2$), the number of infected adult female mosquitoes increases with increasing values of the proportion of newly infected eggs (Figure 9). Figure 9 shows that vertical transmission in the vector population has little or no effect on the number of infected adult female mosquitoes.

5. Sensitivity Analysis

It is necessary to know the relative importance of the different factors responsible for ZIKV transmission and prevalence to find the best ways to reduce population morbidity and mortality. We use sensitivity analysis to determine the robustness of model predictions to parameter value variations. Our goal is to discover the parameters with a high impact on the basic reproduction number, R_0 , that the control strategies should target.

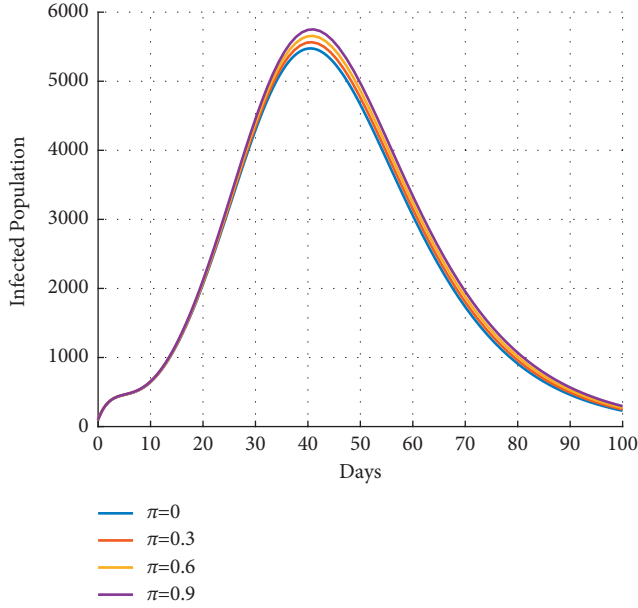


FIGURE 9: Evolution of the epidemic spreading in the vector population for various values of the vertical transmission rate π . Mosquito-to-human interaction is set at $a = 0.2$.

The sensitivity indices inform us about the relative influence of each parameter on disease transmission and prevalence. We derive an analytical expression for the sensitivity of the parameter p using the normalized forward sensitivity index as follows:

$$\Upsilon_p^{R_0} = \frac{\partial R_0}{\partial p} \cdot \frac{p}{R_0}. \quad (15)$$

Results of the sensitivity analysis reported in Table 4 reveal that R_0 is sensitive priority to the parameter values involved in the vector-to-human transmission of ZIKV such as the biting rate (a), transmission probabilities (β_{vh}, β_{hv}), and the mortality rate of adult mosquitos (μ_v). These results indicate that control strategies targeting the vector population may be the most beneficial for reducing R_0 .

To illustrate the influence of the parameters on the basic reproduction number (R_0), we produce the contour plots of R_0 in terms of human-to-vector transmission rate β_{hv} and human-to-human transmission rate β_{hh} in Figure 10. It appears that the simultaneous reduction in human-to-vector transmission rate and human-to-human transmission rate allows controlling the epidemics. However, the most impacted full-control parameter is the human-to-human transmission rate β_{hh} . Indeed, if the rate of sexual transmission is higher than 0.1, reducing the human-to-vector transmission rate has almost no impact on the epidemic.

Figure 11 reports the impact of the human-to-human transmission rate β_{hh} and the mortality rate of adult mosquitos μ_v on the basic reproduction number. It highlights the preponderance of reducing the human-to-human transmission rate to control the epidemic.

Figure 12 relates the number of bites per mosquito per day a and the human-to-human transmission rate β_{hh} to the

TABLE 4: The global sensitivity analysis indicates the sensitivity of the basic reproduction number, R_0 , to the model parameters. Bars indicate partial rank correlation coefficients (PRCCs). It illustrates the contribution of parameters to variability or uncertainty in the model outputs (R_0).

Parameter	Parameter sensitivity index
μ_v	-0.858 597
a	+0.710 061 2
γ_h	-0.614 142 5
μ_h	-0.645 237 5
b	+0.644 969 4
β_{vh}	+0.355 030 6
β_{hv}	+0.355 030 6
ϕ	+0.355 341 6
β_{hh}	+0.289 938 8
α_v	+0.147 929 4
π	+0.000 606 406 7
d	-0.015 353 56
θ	+0.000 606 406 7
α_h	+0.000 148 373 3
μ_e	-0.000 310 977 8

evolution of the basic reproduction number (R_0). Reducing the number of bites per mosquito per day does not allow to control the epidemics when the rate of sexual transmission is higher than 0.1.

Finally, Figure 13 plots the evolution of the basic reproduction number based on variations of the vertical transmission rate π and the human-to-vector transmission rate β_{hv} . It shows that vertical transmission does not impact the epidemic compared to reducing the human-to-vector transmission rate. Note that in these figures, we fix all other parameters to the values given in Table 1.

Unlike alternative models proposed in the literature, we have introduced a model to investigate all the transmission routes. Simulations show that neglecting the secondary transmission channels can lead to a wrong estimation of the peak of the disease in the human population. Additionally, it has a severe impact on the time needed to reach the peak of the disease. Such wrong estimations can lead to inadequate control policies with disastrous consequences on the population's health. Furthermore, simulation performed with realistic parameter values shows that to control the spread of the disease, it is imperative to contain the following parameters simultaneously: the human-to-human transmission rate and the human-to-vector transmission rate below 0.1, or the human-to-human transmission rate and the mosquito bite rate below 0.1 and 0.2, respectively, or to simultaneously control the human-to-human transmission rate and the mortality rate of adult mosquitoes of less than 0.05 and greater than 0.2, respectively.

6. Parameter Estimation and Model Validation: The Colombia Scenario

In this section, we estimate the values of β_{hh} (human-human transmission rate) and π (vertical transmission rate) parameters related to the population dynamics of ZIKV spread through human and mosquito populations.

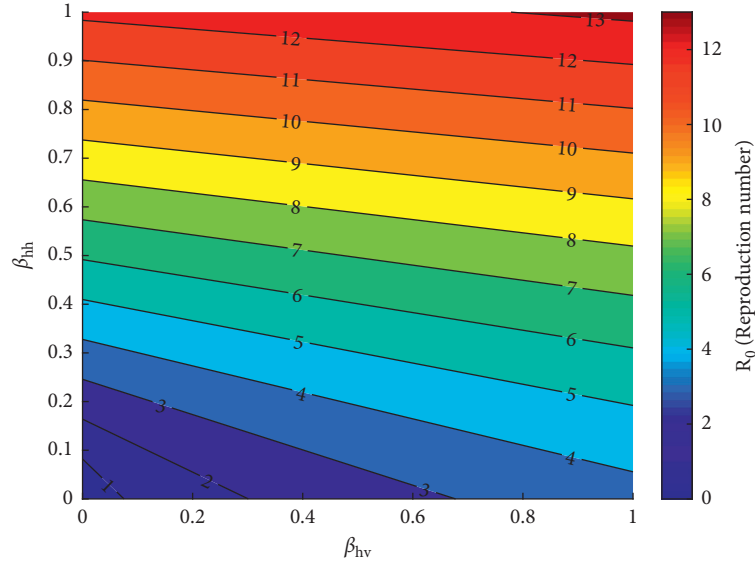


FIGURE 10: The contour plot of the basic reproduction number as a function of the human-to-vector transmission rate (β_{hv}) and the human-to-human transmission rate (β_{hh}).

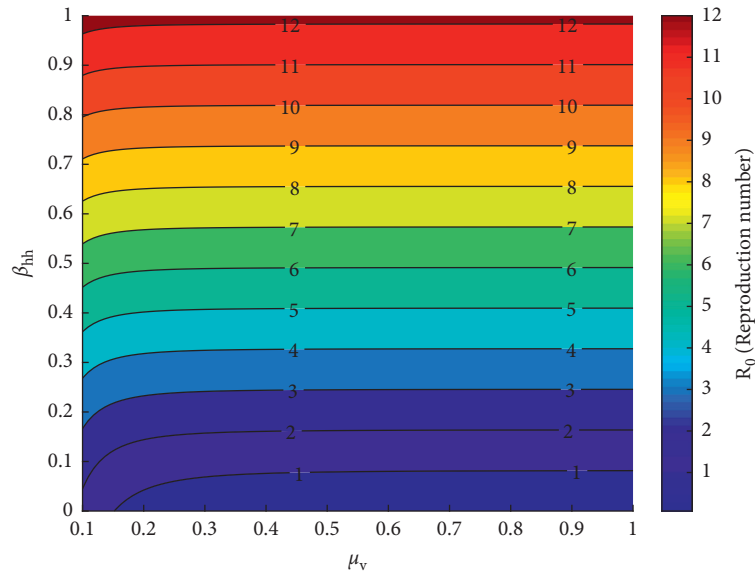


FIGURE 11: The contour plot of the basic reproduction number as a function of the mortality rate of adult mosquitoes (μ_v) and human-to-human transmission rate (β_{hh}).

For the mathematical model of ZIKV (1), some parameter values are known and available in scientific journals. In order to simulate the dynamics of the Zika virus in the Colombian population, it is necessary to identify some of the parameter values of the mathematical model. Thus, the unknown values of the parameters must be estimated using real data regarding the prevalence of the Zika virus. The objective of this section is to explain the behavior of the population-level Zika disease dynamics in Colombia for the year 2016, which also has been used in literature [22]. The Zika prevalence data were collected from the data available from the National Institute of Health in Colombia. In

Table 5, we can see the seroprevalence of Zika disease for different weeks of 2016 in Colombia.

The only parameters we estimated are the human-to-human (β_{hh}) transmission and the vertical transmission rate (π) in mosquitoes. The rest of the parameters remain unchanged. In order to fit the mathematical model (1) of ZIKV to the time-series data of Zika prevalence in Colombia, we found the best-fit model parameters for the considered model (1) with the abovementioned data using MATLAB's `fmincon` minimization software. As indicated in [24], we use a total population of 19,471,223, since this is the number of people living below the 1,400 meters where the mosquitoes

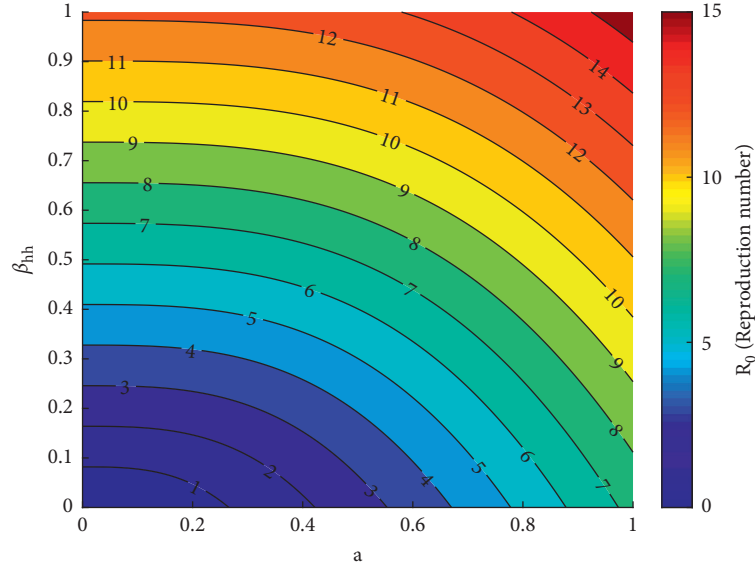


FIGURE 12: The contour plot of the basic reproduction number as a function of the mosquito biting rate. Number of bites per mosquito per day (a) and human-to-human transmission rate (β_{hh}).

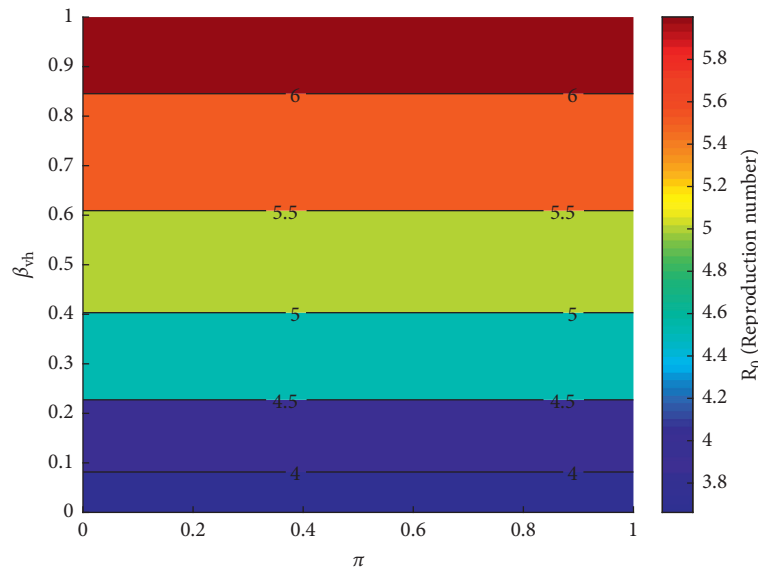


FIGURE 13: The contour plot of the basic reproduction number as a function of the vertical transmission rate (π) and human-to-vector transmission rate (β_{hv}).

that transmit the Zika virus live. In addition, we considered the initial number of infected populations as 2,173 as shown in the data in Table 5. After the estimation, we have the value of the parameters as follows:

$$\begin{aligned} I_h(0) &= 2173, \\ \beta_{hh} &= 0.1, \\ \pi &= 0.2. \end{aligned} \quad (16)$$

In Figure 14, we represented the data on Zika infections in Colombia reported from the first to the thirty-sixth week of 2016 using blue dots. With the estimated

parameters of the model, we predict that the population density stays infected until 80 weeks. According to the prediction of the curve, the disease will no longer break out after 50 weeks in Colombia, which is supported by the actual cases reported in the same region by the WHO [25] and confirmed by [22]. Our model predicts that there will be an average of 137 weekly cases between the 37th and 52nd weeks of 2016, which is near the 130 real cases reported by the WHO [25]. According to our predictive model, Zika will be eradicated from Colombia from week 28 of 2017. This is also supported by the actual data [25]. This confirms the results of [22].

TABLE 5: The weekly reported data of Zika infection cases in Colombia from 1 to 36 weeks of 2016 provided by the National Institute of Health SIVIGILA, which are also used in [23].

Weeks	Cases	Weeks	Cases
1	2173	19	3281
2	4105	20	638
3	4166	21	1567
4	4669	22	2014
5	4198	23	1539
6	4316	24	1344
7	5460	25	1128
8	2865	26	991
9	3767	27	892
10	2655	28	705
11	2639	29	648
12	3882	30	496
13	3808	31	416
14	3059	32	215
15	3364	33	301
16	2671	34	271
17	2665	35	568
18	2687	36	383

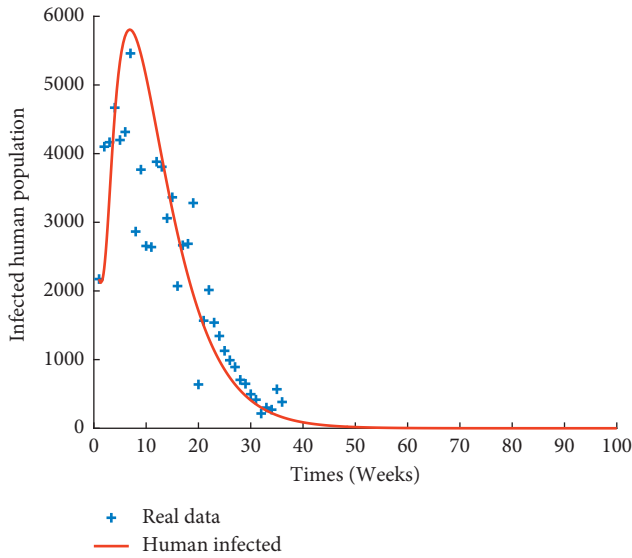


FIGURE 14: Best fit of the ZIKV mathematical model (1) with a scale factor to the time-series data of Zika in Colombia corresponding to the year 2016. The red solid line shows the best model fit.

7. Discussion and Conclusions

This study develops a compartmental model for Zika incorporating human transmission and vertical transmission on mosquitoes. To better understand the effect of additional transmission routes in Zika disease dynamics, we investigate each type of transmission on disease spreading using realistic parameter values. Results show that the maximum number of infected individuals occurs when all transmission routes are considered. Indeed, about 1.5 times more people are infected with ZIKV at the epidemic's peak than in the single-vector model. As illustrated by Figure 3, human-to-human transmission has a significant impact on the initial growth of an epidemic. It results in up to 1.2 times more cases of Zika

at the peak of the outbreak than when one considers the vector transmission model alone. Numerical simulations show that vertical transmission has a negligible effect on the dynamics of disease spreading (see Figure 8). Considering the full model not only increases the maximum number of individuals infected with Zika, but it also increases the speed of the epidemic spreading, with the peak of the epidemic occurring earlier than expected with the alternative models.

In addition, we calculate the basic reproduction number. This quantity allows knowing whether the disease tends to be extinct or becomes an epidemic. Furthermore, we perform a sensitivity analysis to uncover the most influential parameters on the basic reproduction rate.

The sensitivity analysis shows that the mosquito mortality rate, the recovery rate of humans, the biting rates, and the transmission probabilities are the most influential parameters in the development of epidemics. The first two parameters have negative relationships, and the others have positive relationships. In other words, to reduce the number of Zika cases, we need to increase the mortality rate of mosquitoes by controlling mosquito breeding. Second, we need to improve the effectiveness of treatment of the disease and reduce the probability of vector-to-human transmission by protecting ourselves from mosquito bites day and night. The probability of human-to-human transmission also needs to be reduced.

The contour plot simulations also show that, for the disease to disappear, it is imperative to simultaneously control the human-human transmission rate and the human-vector transmission rate each to a value below 0.1. It is also possible to simultaneously control the human-to-human transmission rate and the mosquito bite rate below 0.1 and 0.2, respectively, or simultaneously control the human-to-human transmission rate and the mortality rate of adult mosquitoes less than 0.05 and greater than 0.2, respectively.

In vector transmission models, it is necessary to consider all types of transmission routes to have the most accurate results. Not taking into account the combination of sexual and vertical transmission can lead to poor decisions linked to the disease dynamics. Wrong estimates of the peak of the disease and its timing can have multiple consequences. Assuming that public health officials use predictive modeling tools to determine the timing and intensity of control strategies, the variation in the number of infected persons between the vector-only model and the model used in our study may negatively impact the outcome of these strategies.

The last part of this study is devoted to the numerical simulation of different scenarios based on the official data published by the National Institute of Health-SIVIGILA, Colombia, from the 1st to the 36th week. We estimated by fitting epidemiological parameters such as human and vertical transmissions in mosquitoes using existing discrete real data. Acceptable agreement between data analysis and numerical solutions is established.

This study aims to provide a general overview of the impact of combining a few types of transmission in the spread of ZIKA disease. We use a model that takes into account both human-to-human transmission and vector transmission in mosquitoes. Although the combination of

these two types of transmission accelerates the incidence of ZIKA, it may be necessary to understand the difference between transmission in women and men to examine the risks of infection in both sexes, particularly in pregnant women, which may increase the incidence of secondary infections. In addition, as mosquito population dynamics depend on the season, the effects of seasonality need to be taken into account, as it can affect disease transmission dynamics. We have not yet considered the impact of human mobility on disease spreading. Also since this study focuses on the contribution of Zika transmission pathways to the spread of the disease in the human population, we focused our research on these secondary transmission pathways. In addition, other mathematical analyses such as the existence of an endemic equilibrium, the asymptotic stability of the disease-free and endemic equilibrium points, the bifurcation behavior of the model, and the comparison with a stochastic model should also be explored. All these issues are the subject of future work.

Data Availability

The Zika data used to support the findings of this study are included within the article.

Conflicts of Interest

The authors declare that they have no conflicts of interest.

References

- [1] R. S. Lanciotti, O. L. Kosoy, J. J. Laven et al., "Genetic and serologic properties of Zika virus associated with an epidemic, Yap State, Micronesia, 2007," *Emerging Infectious Diseases*, vol. 14, no. 8, pp. 1232–1239, 2008.
- [2] C.-L. Van-Mai, R. Claudine, T. Anita et al., "Zika virus, French polynesia, South pacific, 2013," *Emerging Infectious Diseases*, vol. 20, no. 6, pp. 1085–1086, 2014.
- [3] Paho Who, "Zika virus infection and Zika fever: frequently asked questions [Internet]," Pan American Health Organization/World Health Organization, Washington D.C, USA, 2016, http://www.paho.org/hq/index.php?option=com_content&view=article&id=9183:2015-preguntas-frecuentes-virus-fiebre-zika&Itemid=41711&lang=en.
- [4] Who, "WHO Director-General summarizes the outcome of the Emergency Committee regarding clusters of microcephaly and Guillain-Barre syndrome [Internet]," 2016, <http://www.who.int/mediacentre/news/statements/2016/emergency-committee-zikamicrocephaly/en/>.
- [5] S. Towers, F. Brauer, C. Chavez-Castillo, A. K. L. Falconar, A. Mubayi, and C. M. E. Vivas-Romero, "Estimate of the reproduction number of the 2015 Zika virus outbreak in Barranquilla, Colombia, and estimation of the relative role of sexual transmission," *Epidemic*, vol. 17, pp. 50–55, 2016.
- [6] D. Soriano-Paños, J. H. Arias-Castro, A. Reyna-Lara, and H. J. Martínez, "Vector-borne epidemics driven by human mobility," *Physical Review Research*, vol. 2, no. 1, Article ID 013312, 2020.
- [7] S. L. Hills, K. Russell, M. Hennessey et al., "Transmission of zika virus through sexual contact with travelers to areas of ongoing transmission - continental United States, 2016," *MMWR Morb Mortal Wkly Rep*, vol. 65, no. 8, pp. 215–216, 2016.
- [8] G. Venturi, L. Zammarchi, C. Fortuna et al., "An autochthonous case of Zika due to possible sexual transmission, Florence, Italy, 2014," *Euro Surveillance*, vol. 21, no. 8, 2016.
- [9] D. Gao, Y. Lou, D. He et al., "Prevention and control of Zika as a mosquito-borne and sexually transmitted disease: a mathematical modeling analysis," *Scientific Reports*, vol. 6, no. 1, pp. 1–10, 2016.
- [10] M. Arquam, A. Singh, and H. Cherifi, "Impact of seasonal conditions on vector-borne epidemiological dynamics," *IEEE Access*, vol. 8, Article ID 94510, 2020.
- [11] P. Suparit, A. Wiratsudakul, and C. Modchang, "A mathematical model for Zika virus transmission dynamics with a time-dependent mosquito biting rate," *Theoretical Biology and Medical Modelling*, vol. 15, no. 1, pp. 1–11, 2018.
- [12] F. B. Augusto, S. Bewick, and W. F. Fagan, "Mathematical model of Zika virus with vertical transmission," *Infectious Disease Modelling*, vol. 2, no. 2, pp. 244–267, 2017.
- [13] E. Chikaki and H. Ishikawa, "VA dengue transmission model in Thailand considering sequential infections with all four serotypes," *Infect. Dev. Countr.*, vol. 3, no. 9, pp. 711–722, 2009.
- [14] M. Andraud, N. Hens, C. Marais, and P. Beutels, "Dynamic epidemiological models for dengue transmission: a systematic review of structural approaches," *PLoS One*, vol. 7, Article ID e49085, 2012.
- [15] A. J. Kucharski, S. Funk, R. M. Eggo, H.-P. Mallet, W. J. Edmunds, and E. J. Nilles, "Transmission dynamics of zika virus in island populations: a modelling analysis of the 2013 + 14 French polynesia outbreak," *PLoS Neglected Tropical Diseases*, vol. 10, Article ID e0004726, 2016.
- [16] A. S. Abdullah and J. Wang, "New mathematical model of vertical transmission and cure of vector-borne diseases and its numerical simulation," *Advances in Difference Equations*, vol. 2018, no. 1, pp. 1–15, 2018.
- [17] A. Sharma and S. K. Lal, "Zika virus: transmission, detection, control, and prevention," *Frontiers in Microbiology*, vol. 8, 2017.
- [18] Y. Dumont, F. Chiroleu, and C. Domerg, "On a temporal model for the chikungunya disease: modeling, theory and numerics," *Mathematical Biosciences*, vol. 213, no. 1, p. 80, 2008.
- [19] C. Burgess, H. Gaff, J. Jackson, and T. Niu, "Mathematical model to assess the relative effectiveness of rift valley fever countermeasures," *International Journal of Artificial Life Research*, vol. 2, no. 2, pp. 1–18, 2011.
- [20] S. T. Pinho, C. P. Ferreira, L. Esteve, F. R. Barreto, V. C. Morato e Silva, and M. G. Teixeira, "Modelling the dynamics of dengue real epidemics," *Philosophical Transactions of the Royal Society of London. Series A. Mathematical, Physical and Engineering Sciences*, vol. 368, no. 1933, pp. 5679–5693, 2010.
- [21] Z. Feng and X. Jorge, "Competitive exclusion in a vector-host model for the dengue fever," *Journal of Mathematical Biology*, vol. 35, pp. 523–5244, 1997.
- [22] S. K. Biswas, U. Ghosh, and S. Sarkar, "Mathematical model of zika virus dynamics with vector control and sensitivity analysis," *Infectious Disease Modelling*, vol. 5, pp. 23–41, 2020.
- [23] G. González-Parra and T. Benincasa, "Mathematical modeling and numerical simulations of Zika in Colombia considering mutation," *Mathematics and Computers in Simulation*, vol. 163, pp. 1–18, 2019.

- [24] Dane Gov, “Departamento administrativo nacional de Estadística, censo Colombia,” 2005, <https://www.dane.gov.co/files/censos/libroCenso2005nacional.pdf>.
- [25] World Health Organization, *Zika-epidemiological Report Barbados, September 2017*, Pan American Health Organization/World Health Organization, Washington, DC, USA, 2017.